UCRL-JC-127880
PREPRINT

Stability of the Graphite and Diamond Phases of Finite Carbon Clusters

N.W. Winter
F.H. Ree

This paper was prepared for submittal to the
Detonation Symposium
Snowmass, CO
August 30-September 4, 1998

August 28, 1998

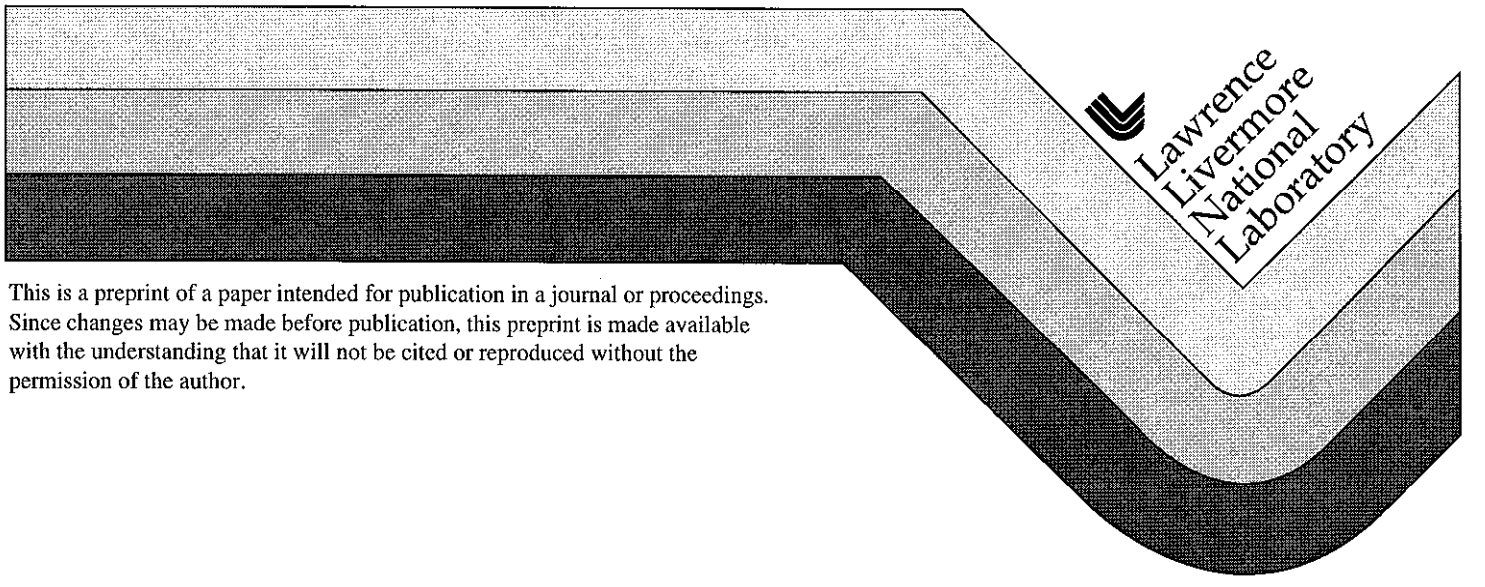

STABILITY OF THE GRAPHITE AND DIAMOND PHASES OF FINITE CARBON CLUSTERS

Nicholas W. Winter and Francis H. Ree
Physics and Space Technology Department
Lawrence Livermore National Laboratory
Livermore, California 94550

The stability of particulate carbon formed in the detonation of high explosives has been investigated with first principles and semiempirical molecular orbital calculations carried out on carbon clusters. The dangling surface bonds were capped with hydrogen atoms and the surface contributions to the cohesive energy were removed by extrapolation as a function of the cluster size. Comparison of the calculated heat of formation of graphite and diamond particles as a function of size predicts that the graphite phase becomes more stable for 10^4-10^5 carbon atoms. Calculations were also carried out on geometry optimized carbon clusters without capping atoms, resulting in reconstructed cluster surfaces that may be a more realistic model for particulate carbon formed under the extreme conditions of detonation. The calculated energy barrier for the conversion of a graphitic cluster to the cubic diamond structure was in good agreement with calculations on bulk graphite.

INTRODUCTION

Solid carbon is a major detonation product of many high explosives (HE). The kinetics of formation and growth of finite carbon particles contribute significantly to the detonation properties of carbon rich CHNO explosives. While nitrogen, oxygen, and hydrogen rapidly form simple molecular detonation products such as N_2, CO_2, and H_2O, carbon forms arbitrarily large molecules and is the only solid detonation product. The relatively slow growth rate of carbon particles gives rise to an extended reaction zone. As a consequence, the detonation is more sensitive to the system configuration, with the observed Chapman-Jouguet (CJ) pressure reflecting the condition of a partially reacted state rather than that of the final detonation products.

The equilibrium carbon phase diagram[1] does not adequately describe particulate carbon, requiring the carbon EOS be adjusted to match the performance of the specific HE being studied. The graphite, diamond, and liquid phases of carbon are usually considered, where graphite and diamond are idealizations of the solid phases formed during detonation. When only graphitic carbon is included, calculations of the detonation velocity for TNT show good agreement for low loading densities ($\rho \leq 1.5$ g/cc), but fail to predict the change in slope of the velocity curve at high densities.[2] Including the diamond phase in the calculations significantly improved the agreement, suggesting that the graphite to diamond phase transformation was responsible. Kerley[2] was able to match the experimental phase transition pressure by assuming imperfections in the diamond phase and adjusting the binding energy. Van Thiel and Ree[3] obtained agreement with the change in slope observed for higher TNT loading densities by increasing the heat of formation of diamond, effectively raising the phase transformation pressure relative to the equilibrium value.[4] They concluded that equilibrium carbon was not a good model for the carbon formed during detonation and suggested that the formation of non-equilibrium carbon clusters could explain the higher phase-transformation pressure.

An accurate model of the effects of particulate carbon on HE performance requires the size dependence of the thermodynamic stability of the different forms of carbon. In this paper several semiempirical and first-principles computational methods for calculating the total energy of a carbon cluster are compared and evaluated. In the next section, the formation of various types of carbon during detonation is reviewed. Following this, previous computational studies of carbon particle stability are discussed and a comparison of the semiempirical and first-principles determination of the cohesive energies of graphite and diamond from small carbon clusters is presented. Finally, an expression for the semiempirical heat of formation as a function of cluster size is used to predict the relative stability of the graphite and diamond phases of finite carbon particles.

CARBON CLUSTER FORMATION IN HE DETONATIONS

The formation of carbon clusters during HE detonations is exothermic, but because the clusters must diffuse together from a large volume, their growth rate is expected to be slow. Shaw and Johnson[5,6] used a diffusion-limited model to demonstrate that carbon clustering is a slow reaction in the detonation regime. Carbon particles were built up from random collisions while the hot dense background fluid maintained the equilibrium temperature, allowing the clusters to anneal to compact spherical objects. The final particle size was estimated to be 10^4-10^5 atoms (50 Å). One of the uncertainties in their model was the size dependence of the cluster energy. They assumed that ΔE, the difference in energy between the cluster and the bulk, was proportional to

the number of surface atoms, leading to $\Delta E_n \propto n^{1/3}$ where n is the number of carbon atoms in the cluster. The model did not distinguish between the various forms of carbon present during the detonation process.

Four types of particles have been identified from recovered detonation soot: amorphous carbon particles, graphite-like particles and ribbons with interplanar disordering, clusters of ultra-dispersed diamond (UDD)[7-10] with grain sizes of 20 to 200 Å, and spherical particles with onion-like structure.[10] Amorphous carbon refers to a disordered network of carbon atoms that have predominantly sp^2 bonding with ~10% sp^3 bonds. Short-range order may be present and varies significantly depending on the preparation. The most important determinants of the short-range order are the ratio of sp^2 to sp^3 bonding and the hydrogen content. Hydrogen satisfies the dangling bonds and allows the sp^2 and sp^3 regions to segregate.

For structures with few atoms, planar graphite is not the most stable sp^2 hybridized form of carbon due to the large number of unpaired surface electrons. Small closed molecules like fullerenes and onions gain stability despite the strain energy associated with the curved surfaces because of the absence of the dangling bonds. Carbon onions are hollow particles consisting of concentric graphite shells with outer diameters ranging from 100 Å to 1 μm and fall in the category of carbon blacks. Onions are significant in the formation of detonation carbon because they allow for the organization of short graphene sheets into compact, dense, three-dimensional structures without dangling bonds. The high pressures associated with detonation should select the denser carbon onions over isolated fullerenes. This has been illustrated in the work of Boese *et al.*[11], who demonstrated the formation of fullerenes in the form of multi-layered onion- and tube-like closed-shell carbons particles following the explosive decomposition of a high energy form of annulene.

The size of the UDD particles implies about 10-20 percent of the atoms are surface atoms. At this point the annealing process stops and further carbon growth is by coagulation of these small clusters, consistent with the diffusion-limited model. Upon heating, the UDD transform to connected planes or closed graphite-like shells. Kuznetsov *et al.*[12] observed that the conversion of diamond to onion-like carbon was from the surface inward and that the transformation temperature was dependent on the particle size. The reverse process, the conversion of onion-like carbon to diamond, was demonstrated by Banhart and Ajayan[13] by heating onion particles to ~700° C, transforming the particle cores to the diamond phase. The compression of the outer layers toward the particle center raised the pressure in the core sufficient for diamond nucleation.

Greiner *et al.*[9] reported that approximately 25 wt% of the recovered soot from an HE detonation is in the form of diamonds with 4-7 nm diameters. The remainder of the soot was composed of disordered graphite ribbons. They argued that the presence of diamond in the recovered soot strongly suggested it is present at the higher temperatures (~3,000 K) and pressures (~300 kbar) of the detonation regime.

Previous Theoretical Studies on Carbon Clusters

Due to the interest in fullerenes, the properties of carbon clusters have been intensively investigated.[7] Based on computational studies, various structures of free clusters, C_n, have been proposed.[14-19] As stated above, the lowest energy state for a cluster with a large number of carbon atoms is three-dimensional planar graphite. For structures with only a few carbon atoms, $n < 20$, the large number of dangling bonds disfavors graphite for one-dimensional polymers and two-dimensional rings. Three-dimensional fullerene cages show a greater stability for $n > 20$. This is despite the strain energy due to the curved surfaces.

In a previous study of carbon clusters, Amlöf and Lüthi[14] carried out large-scale *ab initio* restricted Hartree Fock (RHF) calculations on planar graphene sheets and cubic diamond clusters. The dangling surface bonds were treated either as high-spin coupled singly occupied orbitals or capped with hydrogen atoms. The dependence of the total energy on the number of carbon atoms was obtained by fitting the calculated cluster energies to the equation,

$$E_{tot} = N_C E_C + N_{db} E_{db} \qquad (1)$$

where N_C is the number of carbon atoms, E_C is the energy per carbon atom, N_{db} is the number of dangling bonds, and E_{db} is the contribution to the energy per dangling bond. For the two-dimensional graphite sheets $N_C = 6N^2$ and $N_{db} = 6N$, where N is the number of carbon atoms along one edge. For cubic diamond clusters, $N_C = N(4N^2 - 1)/3$ and $N_{db} = 4N^2$, where N is the number of layers along the c-axis. The fitting coefficients E_{db} and E_C are the contributions to the energy per dangling bond and per carbon atom, respectively.

Neglecting the contribution from the cluster zero-point energy, the cohesive energy is defined as the difference between the total energy per carbon atom and the energy of the free carbon atom. The surface energy contribution becomes less important for larger clusters and the cohesive energy of an infinite cluster can be calculated by referencing E_C to the calculated total energy of atomic carbon. Fitting the high-spin RHF energies from calculations on C_6, C_{24}, and C_{54}, Amlöf and Lüthi[14] predicted the cohesive energy for the infinite graphene sheet to be -125 Kcal/mol. Saturating the dangling bonds with hydrogens, closed-shell RHF calculations on larger clusters with up to 150 carbon atoms were also carried out and gave a slightly lower value for the extrapolated cohesive energy of -124.9 Kcal/mol. The attractive interactions between the layers were estimated to contribute less than 5 Kcal/mol to E_C, and could not account for the sizable disagreement with the experimental value for the cohesive energy of graphite of -169.98 Kcal/mol at T = 0 K.[20] The error was attributed to the electron correlation unaccounted for by the *ab initio* RHF method.

Amlöf and Lüthi[14] also determined the cohesive energies of the three carbon clusters $C_{10}H_{16}$, $C_{35}H_{36}$, and $C_{84}H_{64}$ with the cubic diamond structure and sp^3 bonding. The extrapolated cohesive energy was found to be -124.2 Kcal/mol, considerably smaller than the experimental value for bulk diamond of -169.40 Kcal/mol at T = 0 K,[20] but consistent with the results for graphite discussed above.

Clearly, in order to use total energy cluster calculations to study the relative stability of graphite and diamond clusters as a function of size, it is necessary to find a more reliable method than *ab initio* RHF theory. The next section compares the RHF results to semiempirical and first-principles calculations on larger carbon clusters. By comparing the extrapolated values of the cohesive energies to experiment, the relative accuracy of the methods can be evaluated.

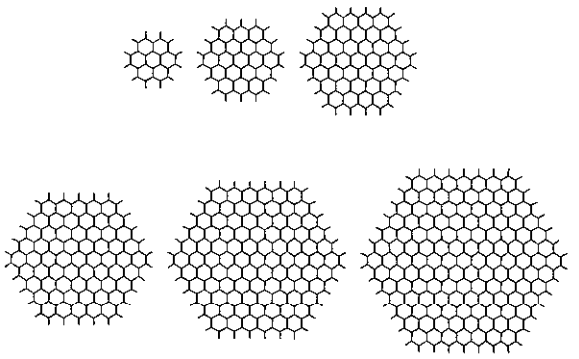

Figure 1. Graphene sheets for N = 2, 3, 4, 5, 6, and 7 corresponding to $C_{24}H_{12}$, $C_{54}H_{18}$, $C_{96}H_{24}$, $C_{150}H_{30}$, $C_{216}H_{36}$, and $C_{294}H_{42}$.

PREDICTION OF DIAMOND AND GRAPHITE COHESIVE ENERGIES FROM CARBON CLUSTER CALCULATIONS

First principles density functional theory (DFT) and semiempirical RHF total energy calculations have been carried out on carbon clusters chosen to mimic the chemical bonding exhibited in the bulk phases of graphite and diamond. The semiempirical MNDO calculations[21] were carried out using the GAMESS[22], HyperChem[23], and SPARTAN[24] molecular electronic structure codes. Both the AM1[25] and PM3[26-28] parameterizations of the MNDO method were tested. The DFT calculations were carried out with the Gaussian 94 molecular orbital program[29] using the Becke[30] hybrid HF exchange and DFT exchange-correlation functional with a 6-31g basis set. Figure 1 shows the $C_{24}H_{12}$, $C_{54}H_{18}$, $C_{96}H_{24}$, $C_{150}H_{30}$, $C_{216}H_{36}$, and $C_{294}H_{42}$ graphene clusters with aromatic sp^2 bonding.

The $C_{10}H_{16}$, $C_{35}H_{36}$, $C_{84}H_{64}$, $C_{165}H_{100}$, and $C_{286}H_{144}$ cubic diamond clusters with sp^3 bonding are given in Figure 2. In each case, the singly occupied surface orbitals are capped with hydrogen atoms. The structures were determined by molecular mechanics energy minimization which gave bond distances close to the experimental values of 1.42 Å for graphite and 1.54 Å for diamond.[7]

The following equation was used to express the total energy per carbon atom as a linear function of the hydrogen to carbon ratio,

$$\frac{E_{tot}}{N_C} = E_C + \frac{N_H}{N_C} E_H \qquad (2)$$

where E_{tot}, E_C, and N_C are as defined for equation 1. N_H is the number of hydrogen atoms used to cap the dangling bonds and is given by the same expression as for N_{db}. The C-H bond energy contribution is given by E_H. The coefficients determined from the least squares fit of E_{tot} as a function of N_H/N_C for the graphite and diamond clusters are given in table 1 for each of the computational methods.

Extrapolation of the PM3 graphene cluster energies predicted a cohesive energy of -166.93 Kcal/mol and the AM1 parameterization gave E_C = -165.94 Kcal/mol. These values differ from the experimental value[20] by only 3.05 and 4.04 Kcal/mol respectively. For the diamond clusters the PM3 method predicted a cohesive energy of -166.95 Kcal/mol and the AM1 method gave -165.23 Kcal/mol. Compared to experiment, the semiempirical diamond cohesive energies are too high by 2.45 and 4.17 Kcal/mol respectively. In either case, the semiempirical results are considerably more accurate than the *ab initio* RHF calculations[14] which extrapolated to E_C = -124.21 Kcal/mol.

Since E_C for graphene given in table 1 does not include the attractive dispersion energy between the sp^2 planes, the extrapolated cohesive energy for three-dimensional planar graphite will be ~1 Kcal/mol lower than the single sheet values. After including the dispersion interaction, each of the methods predicts the correct order for bulk graphite and diamond stability.

The first-principles DFT method provides another approach to study the phase stability of particulate carbon. In order to make a comparison to the *ab initio* and semiempirical RHF methods, DFT calculations were carried out for the smallest three sp^2 and sp^3 clusters using the Gaussian 94 program.[30] For graphite, DFT predicted E_C = -167.78 Kcal/mol and for diamond, E_C = -155.43 Kcal/mol. The magnitudes of the DFT cohesive energies are in closer agreement with experiment than were the *ab initio* RHF results, but the relative energies of the two phases are in far worse agreement. The 6-31G basis set may have been too small and the DFT calculations are being repeated with larger basis sets in order to check the accuracy of these results.

The semiempirical RHF method gave the best agreement with experiment. This is due in part to the fact that the AM1 and PM3 parameters were fitted to the experimental enthalpy of formation of organic compounds, making them well suited to the calculation of the cluster cohesive energies depending primarily on the formation of C-C and C-H bonds.

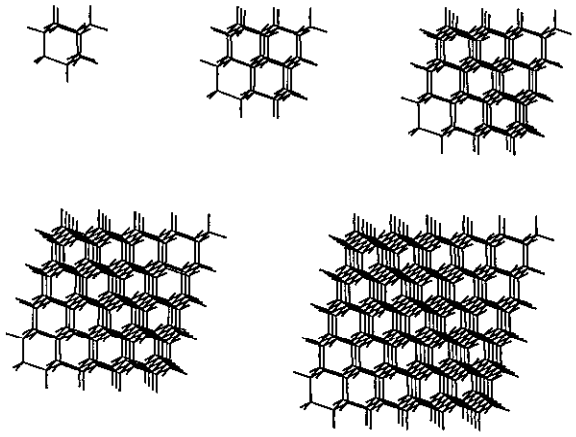

Figure 2. Cubic diamond clusters for N=2, 3, 4, 5, and 6 corresponding to $C_{10}H_{16}$, $C_{35}H_{36}$, $C_{84}H_{64}$, $C_{165}H_{100}$, and $C_{286}H_{144}$.

The parameters incorporate electron correlation and vibrational zero-point corrections that the *ab initio* RHF method neglects. In addition, it is straight forward to adjust the semiempirical parameters to improve the predictions for the experimental conditions of detonation.

Table 1. Energy coefficients determined from the least squares fit of E_{tot} as a function of N_H/N_C for the graphite and diamond clusters given in Figures 1 and 2. The units are Kcal/mol.

	Graphite		Diamond	
Method	E_C	E_H	E_C	E_H
RHF[a]	-124.90	-357.08	-124.21	-360.54
AM1	-165.94	-315.88	-165.23	-320.84
PM3	-166.93	-353.08	-166.95	-358.07
DFT	-167.78	-371.48	-155.43	-387.01

[a]Reference 14

Structural Effects of Surface Bonding

The results discussed above were obtained for molecular mechanics optimization of the cluster geometry after capping the dangling bonds with hydrogen. This gave C-C bond distances close to the experimental graphite distance of 1.42 Å. Optimization of the capped clusters using the semiempirical RHF method gave essentially the same results with a slight shortening of the C-C bonds at the edges of the cluster. If the surface orbitals are left uncapped, the finite graphene sheets distort due to bond formation between adjacent pairs of adjacent planar-dangling orbitals. The AM1 RHF optimized C_{24} cluster is shown in Figure 3.

The locations of the six in-plane π bonds formed by the 12 dangling bonds are shown by the double lines. The out of plane aromatic πbonds are not shown. The additional in-plane π bonding results in a singlet closed-shell cluster. The calculated bond distances for the new C-C bonds are 1.24 Å, indicating an increase in the bond order and the formation of triple bonds. Amlöf and Lüthi[14] found the triple bond distance of C_{24} to be 1.20 Å using the *ab initio* RHF method. The remaining edge bond distances are 1.37 Å and the distances between the carbons forming the interior six member ring are 1.45 Å, slightly longer than for the $C_{24}H_{12}$ capped cluster. The distance between the interior and edge carbons is 1.49 Å. Optimization using the AM1 unrestricted Hatree Fock (UHF) method, increased the bond distance of the short edge bonds to 1.31 Å.

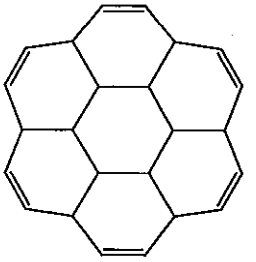

Figure 3. The C_{24} graphene cluster after geometry optimization. The six additional in-plane π bonds formed from the 12 dangling bonds are indicated. The delocalized aromatic π bonds perpendicular to the molecular plane are not shown.

UHF AM1 optimization of the N=3 graphene sheet with 54 carbons gives the structure shown in Figure 4. As was found for C_{24}, 12 of the 18 dangling bonds form six in-plane π bonds shown by the double lines. The calculated bond distances are 1.31 Å, similar to the UHF values for C_{24}. The locations of the remaining six dangling bonds, coupled to give an overall singlet state, are also shown. Amlöf and Lüthi[14] coupled the dangling orbitals to the high-spin value, S=3, in their *ab initio* RHF calculations on the C_{54} cluster. The S=0 AM1 UHF calculations gave a spin-density distribution similar to the S=3 RHF calculations, with the spin-density localized on the carbon atoms.

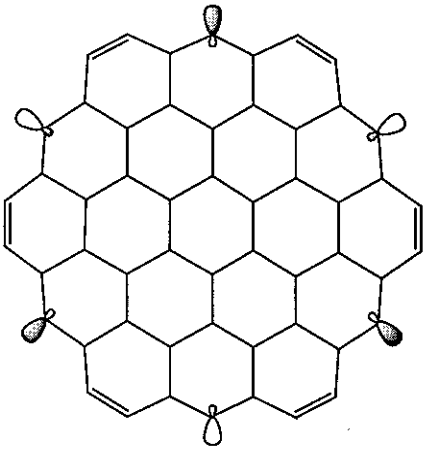

Figure 4. The C_{54} graphene sheet after geometry optimization showing the six additional in-lane π bonds formed from 12 of the original 18 dangling bonds and the locations of the remaining six open-shell orbitals.

The bond distances to the carbons on either side of the singly occupied orbitals were 1.37 Å and the remaining edge bond distances were 1.39 Å. UHF AM1 and PM3 calculations on the larger graphene clusters showed the same surface reconstruction trends.

The molecular mechanics optimized diamond clusters capped with hydrogen atoms, gave $C(sp^3)$-$C(sp^3)$ bond

lengths very close to the experimental value of 1.54 Å. Without the capping atoms, the surface atoms should distort to increase the 2pπ-2pπ overlap, allowing the formation of double bonds and reducing the number of dangling bonds. The surface atoms distort the normal corrugation of the sp^3 bonded planes in order to increase the 2pπ orbital overlap on adjacent carbons. The rounding of the diamond surface elongates the bonds connecting the surface and interior atoms. As discussed below for the larger clusters, this leads to a segregation of the surface and the core atoms resulting in a structure reminiscent of onion-like carbon described above.

The C_{10}, C_{35}, C_{84}, and C_{165} diamond clusters were reoptimized without the capping hydrogen using the semiempirical UHF method with S=0. All the atoms of the C_{10} cluster are on the surface and optimization of the structure for the singlet electronic state lead to a variety of structures. One example is the cage-like molecule with 8 single and 4 double bonds shown in Figure 5. The 16 dangling bonds are reduced to 8, which are associated with the four carbons with only two C-C bonds each.

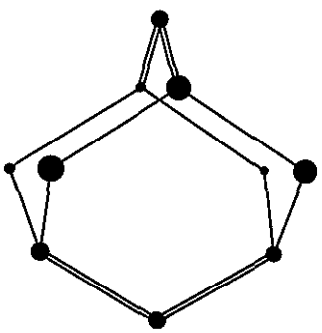

Figure 5. The C_{10} diamond cluster after geometry optimization showing the four double bonds formed from 8 of the original 16 dangling bonds.

The C_{35} cluster has only one interior atom, and optimization of this structure gave a somewhat rounded molecule with significant lengthening of the four bonds to the interior carbon (R_{CC} ~2.2 Å). The surface carbons formed 4 six-member rings with C-C distances consistent with sp^2 aromatic π bonds. The C_{35} aromatic surface bonds are indicated by double lines in Figure 6.

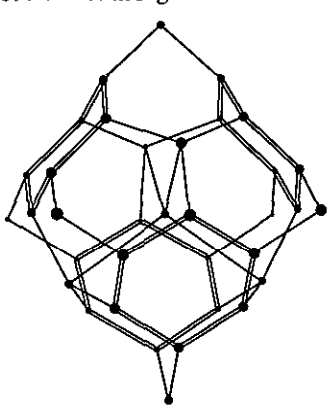

Figure 6. The C_{35} diamond cluster after geometry optimization showing the four aromatic rings formed on the surface.

They account for 24 of the original 36 dangling bonds. The remaining 12 dangling bonds are associated with the six carbons having only two C-C bonds each. The central carbon and its four nearest-neighbors all have four sp^3 bonds.

Optimizing the geometry of the C_{84} cluster without hydrogen on the surface leads to a separation of the 74 carbons on the surface from the C_{10} core, similar to the formation of elongated bonds to the central carbon in the C_{35} cluster. In the case of C_{84} the elongation was more pronounced with some bond distances increasing to more than 3 Å. This is a consequence of the flattening of the surface corrugation in order to form π bonds from the dangling orbitals. Figure 7 shows the similar behavior of the optimized C_{165} cluster. The C_{35} core is indicated by the dashed bonds.

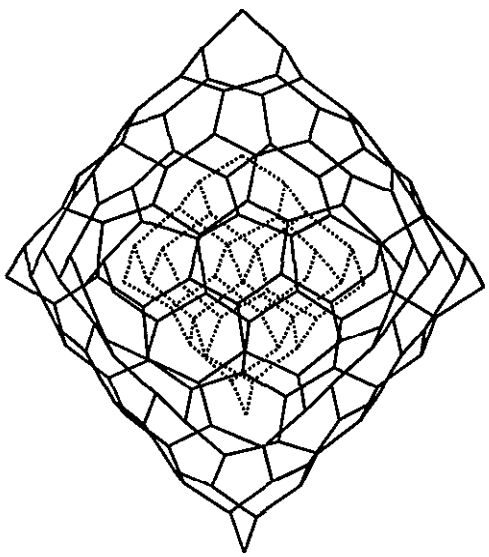

Figure 7. Optimized C_{165} diamond cluster showing the bonds between the 130 surface atoms as single lines and those between the 35 atoms in the core as dashed lines. For clarity the elongated bonds between the surface and core atoms are not shown.

Dependence of the Heat of Formation on Cluster Size

Each carbon atom in graphite forms three intralayer sp^2 bonds and experiences a weak interlayer dispersive interaction with nearest-neighbor graphene sheets. In the diamond lattice each carbon forms four identical sp^3 bonds with the nearest-neighbor carbons. The heats of formation for sp^2 and sp^3 carbon clusters can be expressed in terms of the CC and CH bond energies and the atomic heats of formation. After dividing each equation by the number of carbon atoms, the following linear relationships between the heats of formation and the number of surface bonds per carbon are obtained,

$$\frac{\Delta H_f^0(sp^2)}{N_C} = \frac{3}{2}E_{CC}^{sp^2} + \frac{N_H}{N_C}\left(E_{CH}^{sp^2} - \frac{1}{2}E_{CC}^{sp^2} + \Delta H_f^0(\mathrm{H})\right) + \Delta H_f^0(\mathrm{C}) + \frac{1}{2}E_{disp} \qquad (3)$$

$$\frac{\Delta H_f^0(sp^3)}{N_C} = 2E_{CC}^{sp^3} + \frac{N_H}{N_C}\left(E_{CH}^{sp^3} - \frac{1}{2}E_{CC}^{sp^3} + \Delta H_f^0(\mathrm{H})\right) + \Delta H_f^0(\mathrm{C}) \quad (4)$$

N_C is the number of carbon atoms, N_H is the number of hydrogen atoms, E_{CC} is the energy of the carbon-carbon bond, E_{CH} is the energy of the carbon-hydrogen surface bond, and E_{disp} is the carbon-carbon pair energy due to the interlayer interaction. Using three-dimensional graphite clusters and a model potential[31] for the dispersive attraction between aromatic rings, the latter has been calculated to be 1.66 Kcal/mol.

Equating the intercepts to the experimental cohesive energies of graphite and diamond gives the following estimates for the bond energies (in units of Kcal/mol),

$$E_{CC}^{sp^2} = -\frac{2}{3}\Delta H_f^0(\mathrm{C}) + 0.83 = -114.75$$

$$E_{CC}^{sp^3} = -\frac{1}{2}\Delta H_f^0(\mathrm{C}) + 0.45 = -85.42$$

where 0.45 Kcal/mol is the standard heat of formation of bulk diamond at T=298.15 K and the heat of formation of carbon is 171.29 Kcal/mol.[20] The CH bond energies were determined by fitting the semiempirical AM1 and PM3 cluster calculations, giving the following values for the two semiempirical methods (in units of Kcal/mol),

$$E_{CH}^{sp^2}(AM1) = -110.44, E_{CH}^{sp^3}(AM1) = -100.55$$

$$E_{CH}^{sp^2}(PM3) = -99.20, E_{CH}^{sp^3}(PM3) = -109.83$$

Figure 8 compares heats of formation determined from equations (3) and (4) to the AM1 semiempirical HF cluster calculations. For small clusters the diamond form is more stable due to the greater number of CH bonds. The graphite structure becomes more stable for clusters with approximately 70,000 atoms. The PM3 calculations give similar curves which cross for clusters with approximately 33,000 carbon atoms. While the predictions based on the two methods differ by a factor of two, both results are the same order of magnitude as the observed grain sizes of diamonds recovered from detonation soot.

If the dangling bonds are not capped with hydrogen atoms, equations 3 and 4 can still be used to predict the dependence of the heat of formation on cluster size if E_{CH} is replaced by energy contribution per dangling bond, E_{db}. The latter can be determined by fitting the energies of optimized carbon clusters such as those shown in Figures 3-7. In this case the sp^3 structures are less stable than the sp^2 structures for all cluster sizes and there is no curve crossing. As discussed above, the uncapped clusters are not pure sp^3 or sp^2 due to surface reconstruction. The cluster bonding approaches that of diamond or graphite as the number of atoms increases.

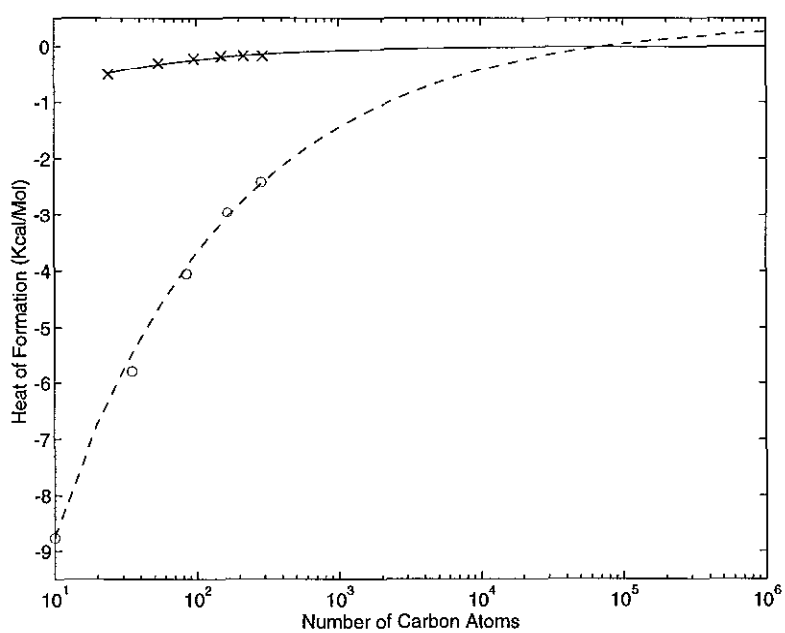

Figure 8. Comparison of the cluster size dependence of the heat of formation for sp^3 (o) and sp^2 (x) clusters determined by the AM1 HF method. The fits to the data are given by the dashed (sp^3) and solid lines (sp^2).

GRAPHITE-DIAMOND PHASE TRANSFORMATION FOR CARBON CLUSTERS

The investigation of the dynamics of the graphite-diamond phase transformation for carbon clusters is extremely complex. The potential energy hypersurface describing the energetics of the conversion from sp^2 to sp^3 bonding involves a large number of degrees of freedom, making it difficult to locate the transition state. In addition, the finite size of the clusters leads to a relatively large contribution from the dangling surface bonds which may (a)

enhance the cluster reactivity and bind free radicals such as H, N, O, NO, or OH present during the detonation, (b) form intramolecular surface bonds (*e.g.* converting sp^2 bonding to sp at the surface of graphite or sp^3 to sp^2 at the surface of diamond), and (c) lead to changes in spin coupling during the course of the phase transformation.

DFT, *ab initio* unrestricted Hartree Fock (UHF), and semiempirical UHF calculations of the energy along a model reaction path for the graphite-diamond transformation of small carbon clusters have been carried out. The model reaction path was defined by the linear synchronous transit (LST) approximation which assumes the intermediate points are linear interpolations between the reactant and product structures. In this approximation all atoms move synchronously along a coordinate in hyperspace and the point of maximum energy is an approximation to the transition state for the reaction. The LST reaction coordinate is not the minimum energy path, but defines a consistent reaction path that can be used to compare the various electronic structure methods.

The initial, final, and transition state structures along the LST reaction coordinate describing the transformation of a rhombohedral graphite cluster containing 140 carbons and 60 dangling bonds to a cubic diamond cluster with 90 dangling bonds are shown in Figure 9. The structures of the initial (100% sp^2) and final (100% sp^3) clusters were determined by molecular mechanics optimization. For the sp^3 cluster this gave a C-C bond length of 1.53 Å and an out-of-plane corrugation is 0.255 Å. For the sp^2 cluster, the C-C bond length was 1.41 Å and the distance between the aromatic planes was 3.3 Å.

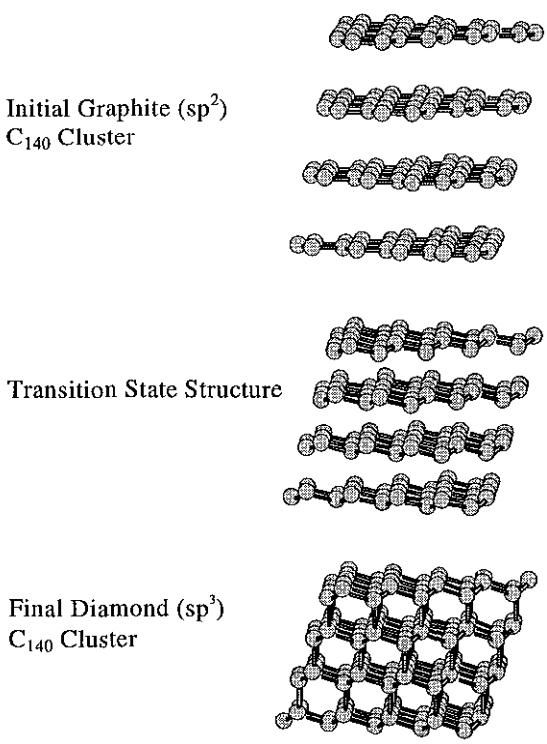

Figure 9. The C_{140} graphite, transition state, and diamond clusters for the LST reaction coordinate.

The LST AM1 C_{140} cluster energies are compared the local density (LDA) calculations of Fahy, *et al.*[32,33] in Figure 10. The reaction path for the LDA calculations was defined by systematically decreasing the interplanar distance of periodic rhombohedral graphite and allowing the other distances and angles to optimize. As expected, the LDA curve is much softer in the graphitic region from 3.3 to 2.5 Å, since the LST reaction coordinate overestimates the in-plane changes as the *c*-axis distance is reduced. The periodic LDA calculations do not have dangling bonds, and the difference in the two curves in the diamond region (interplanar distance < 2 Å) is due to the 30 additional dangling bonds for the sp^3 cluster compared to the sp^2 reference cluster. Considering the differences in the reaction paths and methods being compared, the agreement in the shape and location of the energy barrier is excellent. The difference between the barrier heights is primarily due to the surface bonds of the finite cluster.

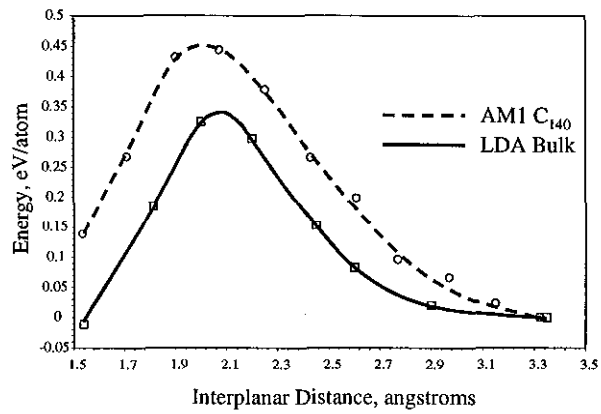

Figure 10. Comparison of the bulk LDA[32,33] and the C_{140} LST reaction energies.

Summary

Ab initio and semiempirical molecular orbital HF calculations have been carried out on carbon clusters representing graphite and diamond particles. The singly occupied surface orbitals were capped with hydrogen atoms in order to enforce the carbon atom hybridization at the surface. Finite size effects were removed by extrapolating the cluster energies as a function of the hydrogen to carbon ratio. The PM3 and AM1 semiempirical cluster energies predicted bulk cohesive energies with 3-4 Kcal/mol of the zero-temperature experimental values. *Ab initio* HF results[14] were considerably less accurate differing by over 45 Kcal/mol from experiment.

The carbon cluster heat of formation as a function of size was determined using the experimental cohesive energies of diamond and graphite along with the calculated C-H bond energies of the hydrogen capped clusters. These results predict that diamond clusters larger than 30,000-70,000 atoms become less stable than graphite clusters of the same size.

Calculation of the energy barrier for the graphite to diamond transformation for finite carbon clusters gave good agreement with first principles calculations on bulk carbon.[32,33] The barrier height was not found to be relatively insensitive to the cluster size.

ACKNOWLEDGEMENTS

This work was performed under the auspices of the U.S. Department of Energy by Lawrence Livermore National Laboratory under contract No. W-7405-Eng-48 and funded by the Accelerated Strategic Computing Initiative (ASCI).

REFERENCES

1. Bundy, F. P., J. Chem. Phys., 41 (1964) 3809.

2. Kerley, G. I., in Short, J. (Ed) Proceedings of the Eighth Symposium (International) on Detonation, NSWC MP 86-194, Naval Surface Weapons Center, White Oak, MD, 1987, p. 540.

3. van Thiel, M. and Ree, F. H., J. Appl. Phys., 62 (1987) 1761.

4. Bundy, F.P., J. Geophy. Res., 85B (1980) 6930.

5. Johnson, J. D. and Shaw, M. S., Schmidt, S. C., Dick, R. D., Forbes, J. W., and Tasker, D. G. (Eds),in Shock Compression of Condensed Matter-1991, Elsevier Science Publishers B. V., 1992, p. 333.

6. Shaw, M. S. and Johnson, J. D., J. Appl. Phys., 62 (1987) 2080.

7. Dresselhaus, M. S., Dresselhaus, G., and Eklund, P. C., Science of Fullerenes and Carbon Nanotubes, Academic Press, San Diego, 1995.

8. Badziag, P., Werwoerd, W. S., Ellis, W. P., and Greiner, N. R., Nature, 343 (1990) 244.

9. Greiner, N. R., Phillips D. S., Johnson J. D., and Volk, F., Nature, 333 (1988) 440.

10. Mal'Kov, I. Y. and Titov, V. M., in Schmidt, S. C. and Tao, W. C. (Eds), Shock Compression of Condensed Matter-1995, AIP Press, American Institute of Physics, AIP Conference Proceedings 370 Part 2, 1996, p783.

11. Boese, R., Matzger, A. J., and Vollhardt, P. C., J. Am. Chem. Soc., 119 (1997) 2052.

12. Kuznetsov, V. L., Chuvilin, A. L., Butenko, Y. V., Mal'Kov, I. Y., and Titov, V. M., Chem. Phys. Lett., 209 (1994) 72.

13. Banhart, F. and Ajayan, P. M., Nature, 382 (1996) 433.

14. Amlöf, J. and Lüthi, H.P., in Jensen, K. F. and Truhlar, D. G. (Eds) ACS Symposium Series: Supercomputer Research in Chemistry and Chemical Engineering, American Chemical Society, Washington, 1987.

15. Parasuk, V. and Amlöf, J., J. Chem. Phys., 91 (1989) 1137.

16. Parasuk, V., Amlöf, J., and Feyereisen, M., J. Am.Chem. Soc., 113 (1991) 1049.

17. Parasuk, V. and Amlöf, J., Theor. Chim. Acta, 83 (1992) 227.

18. Ritchie, J., King, H., and Young, W., J. Chem. Phys., 85 (1986) 5175.

19. Grossman, J. C., Mitas, M., and Raghavachari, K., Phys. Rev. Lett., 75 (1995) 3870.

20. CRC Handbook of Chemistry and Physics 65th Edition, Weast, R. C., (Ed.), CRC Press, Inc., Boca Raton, 1984-1985, p. D58.

21. M.J.S. Dewar, W. Thiel, J. Am. Chem. Soc., 99 (1977) 4899.

22. Schmidt, M., Baldridge, K., Boatz, J., Elbert, S., Gordon, M., Jensen, J., Koseki, S., Matsunaga, N., Nguyen, K., Su, S., Windus, T., Dupuis, M., and Montgomery, J., J. Comput. Chem. 14, (1993) 1347

23. HyperChem Release 4 for Windows, Hypercube, Inc., Waterloo, Ontario, Canada.

24. Spartan, Version 5.0, Wavefunction Inc., Irvine, CA 92715.

25. M.J.S. Dewar, E.G. Zoebisch, E.F. Healy, J.J.P. Stewart, J.Am. Chem. Soc., 107 (1985) 3902.

26. Stewart, J. J. P., J. Comput.Chem., 10 (1989) 209.

27. Stewart, J. J. P, J. Comput.Chem., 10 (1989) 221.

28. Stewart, J. J. P, J. Comput.Chem., 12 (1991) 320.

29. Gaussian 94, Revision B.1, Frisch, M. J., Trucks, G. W., Schlegel, H. B., Gill, P. M. W., Johnson, B. G., Robb, M. A., Cheeseman, J. R., Keith, T., Petersson, G. A., Montgomery, J. A., Raghavachari, K., Al-Laham, M. A., Zakrzewski, V. G., Ortiz, J. V., Foresman, J. B., Cioslowski, J., Stefanov, B. B., Nanayakkara, A., Challacombe, M., Peng, C. Y., Ayala, P. Y., Chen, W., Wong, M. W., Andres, J. L., Replogle, E. S., Gomperts R., Martin, R. L., Fox, D. J., Binkley, J. S., Defrees, D. J., Baker, J., Stewart, J. P., Head-Gordon, M., Gonzalez, C., and Pople, J. A., Gaussian, Inc., Pittsburgh PA, 1995.

30. Becke, A., J. Chem. Phys. 98, (1993) 5648.

31. Jorgensen, W. L. an d Severance, D. L., J. Am. Chem. Soc., 112 (1990) 4768.

32. Fahy S., S. G. Louie, M. L. Cohen, Phys. Rev. B34, 1191 (1986)

33. Fahy S., S. G. Louie, M. L. Cohen, Phys. Rev. B35, 7623 (1987)